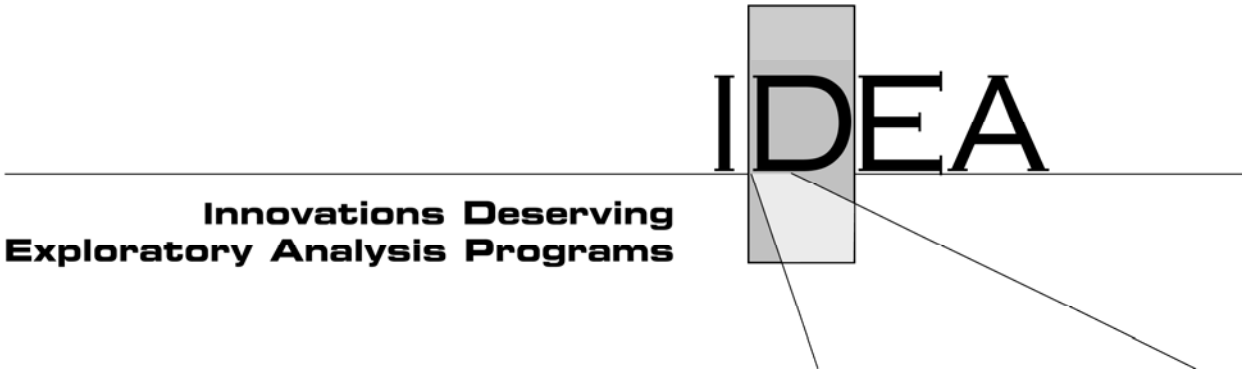

High-Speed Rail IDEA Program

ASSESSMENT OF LASER OPTICS OPEN-AIR COMMUNICATION SYSTEM FOR RAILROADS AND HIGHWAYS

Final Report for High-Speed Rail IDEA Project HSR-3

Prepared by:
Dr. Sheldon S.L. Chang
Electrical Engineering Department, Stony Brook, NY

December 1998

TRANSPORTATION RESEARCH BOARD
OF THE NATIONAL ACADEMIES

INNOVATIONS DESERVING EXPLORATORY ANALYSIS (IDEA) PROGRAMS MANAGED BY THE TRANSPORTATION RESEARCH BOARD

This investigation was performed as part of the High-Speed Rail IDEA program supports innovative methods and technology in support of the Federal Railroad Administration's (FRA) next-generation high-speed rail technology development program.

The High-Speed Rail IDEA program is one of four IDEA programs managed by TRB. The other IDEA programs are listed below.

- NCHRP Highway IDEA focuses on advances in the design, construction, safety, and maintenance of highway systems, is part of the National Cooperative Highway Research Program.
- Transit IDEA focuses on development and testing of innovative concepts and methods for improving transit practice. The Transit IDEA Program is part of the Transit Cooperative Research Program, a cooperative effort of the Federal Transit Administration (FTA), the Transportation Research Board (TRB) and the Transit Development Corporation, a nonprofit educational and research organization of the American Public Transportation Association. The program is funded by the FTA and is managed by TRB.
- Safety IDEA focuses on innovative approaches to improving motor carrier, railroad, and highway safety. The program is supported by the Federal Motor Carrier Safety Administration and the FRA.

Management of the four IDEA programs is integrated to promote the development and testing of nontraditional and innovative concepts, methods, and technologies for surface transportation.

For information on the IDEA programs, contact the IDEA programs office by telephone (202-334-3310); by fax (202-334-3471); or on the Internet at http://www.nationalacademies.org/trb/idea

IDEA Programs
Transportation Research Board
500 Fifth Street, NW
Washington, DC 20001

ASSESSMENT OF LASER OPTICS OPEN-AIR COMMUNICATION SYSTEM FOR RAILROADS AND HIGHWAYS

IDEA Program Final Report
HSR-3

Prepared for
the IDEA Program
Transportation Research Board
National Research Council

Dr. Sheldon S.L. Chang
Electrical Engineering Department
State University of New York
Stony Brook, NY 11794-2350

December 15, 1998

TABLE OF CONTENTS

LIST OF FIGURES

1. EXECUTIVE SUMMARY

The objective of this project was to investigate whether a laser optics open-air communication (LOOC) system can be used as a communication link between a moving train and fixed wayside terminals. The results of this concept evaluation indicate that this technology has real potential for such applications.

There is an increasing need for the rapid exchange of large data files between high-speed trains and wayside facilities. One example is the data exchange requirements of communications-based train control systems. These systems require downloading and uploading of large data files such as track and route characteristics, and train consist data. Another example is the need to exchange health monitoring and diagnostic data. Conventional data radio links may not always be the most effective means for such data exchanges, due to factors such as data volume, interference, and communications coverage problems.

To counteract the undesirable effects of beam deflection by rain drops, snow flakes, etc., we chose to use a diversified laser beam at the sending end and curved reflectors to concentrate the light signal energy to the photo-diodes at the receiving end. The unforeseen dividends are:

(a) that the weak diversified light beam should not pose a health hazard for human eyes, and

(b) that communication reliability should not be compromised by the train's vibrations.

A prototype system was built and successfully demonstrated in a laboratory environment. Further exploration of this concept will require test and evaluation in a railroad operating environment. This testing should include collection of system performance data in a variety of railroad operating and weather environments, e.g., various train speeds and heavy precipitation.

To match the high data transmission rate of the LOOC system to that of the serial data links of the train and wayside computers, a data store and forward computer will have to be developed. The same computer will be used for transmission control, error detection encoding, and retransmission whenever an error is detected.

In working with the Long Island Railroad (LIRR), we realized that the communication data rate of the existing train and wayside computers are in the range of approximately 2×10^4 bits/second while the LOOC data rate is well above 2×10^7 bits/second. Direct use of the LOOC terminals on the train and wayside computers would limit the LOOC transmission capability to one thousandth of what it can do.

Such a computer should be capable of being used with any existing train and wayside computer without modification, or any such computers the railroad may choose to use in the future, to transmit information at full LOOC capacity.

In the following sections the detailed developments of the LOOC automated train control and communication system (LATCC) will be described.

2. LATCC OVERALL SYSTEM DESIGN

Figure 2.1 illustrates a top view of the overall arrangement of the LATCC system. The train terminal

(TT) and wayside terminal (WST) are installed at the same height, about 3 meters, such that two conditions are met:

(i) The train terminal would clear the railway infrastructure.

(ii) The laser beams are too high to impact directly on human eyes.

Condition (ii) is a redundant safety feature. The laser beams are sufficiently weak to be harmless at a distance of two meters or more.

Communication takes place entirely during the train's approach to the wayside terminal. Let x_1 denote the distance between the train and wayside terminals when the communication first starts, and let x_2 denote the distance between the terminals when communication ends. Let y denote the perpendicular distance. Then C, the information transmission capacity in bytes per encounter, is given by:

$$C = \frac{(x_2 - x_1)R}{V} \tag{2.1}$$

where R is the data transmission rate in bytes per second and V is the train velocity in meters per second.

The beam directions of both TT and WST are servo-controlled such that the following conditions are met:

(i) For each terminal, the direction of the laser transmitting beam and direction of the receiving beam, i.e., the direction of maximum receiving sensitivity, are aligned.

(ii) Each receiving beam seeks out and locks onto the direction of maximum incoming signal strength.

In order to satisfy condition (ii), the required beam movement δ during the communication interval is given by:

$$\delta = \tan^{-1}\frac{y}{x_1} - \tan^{-1}\frac{y}{x_2} \tag{2.2}$$

Example 2.1

Given the following data, determine C and δ:

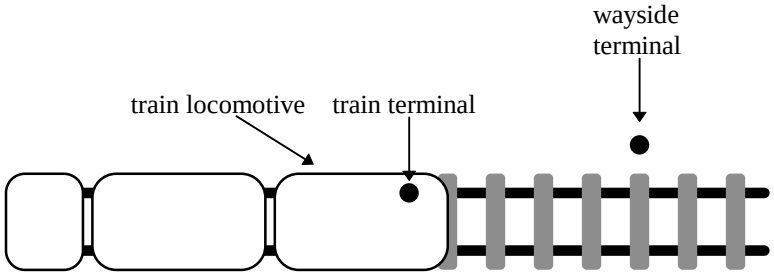

FIGURE 2.1 Top view of LATCC train and wayside communication terminals.

$x_1 = 30$ m
$x_2 = 10$ m
$y = 1$ m
$R = 2 \times 10^6$ bytes / sec
$V = 60$ km / hour

Solution

$$C = \frac{(30 - 10) \times 2 \times 10^6}{60 \times \frac{10^3}{3600}} = 2.4 \times 10^6 \text{ bytes}$$

$$\delta = \tan^{-1}\frac{1}{10} - \tan^{-1}\frac{1}{30} = 5.71^\circ - 1.91^\circ = 3.8^\circ$$

3. MECHANICAL CONSTRUCTION

Figure 3.1 illustrates a train (or wayside) terminal, including a wind resistant external enclosure and vibrational isolation mounting. The train terminal is connected to its communication computer through a co-axial cable. The various components of the train terminal are marked as follows:

(1) photo-optic assembly.

(2) servomotors.

(3) circular windows on the photo-optic assembly.

(4) circular windows on the external enclosure.

(5) part of the electronic assembly. The other part is mounted directly on 1, and is not shown here.

(6) Aeroflex isolators. Two isolators are mounted along the near side between 8 and 9. Two isolators are mounted along the far side between 8 and 9.

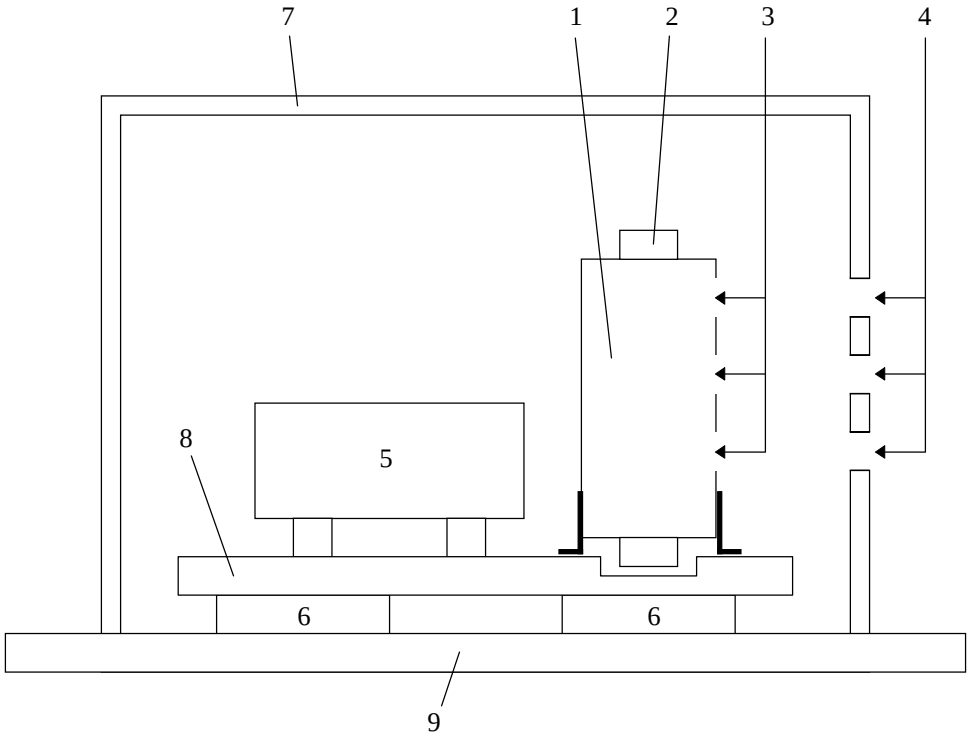

FIGURE 3.1 LATCC terminal construction.

(7) external enclosure.

(8) internal mounting board.

(9) base board.

The train terminal is to be mounted on top of a locomotive while the wayside terminal is to be suspended from an upper structure. The mechanical construction of the photo-optic assemblies are detailed in Section 3.2.

Figure 3.2 illustrates the photograph of a shock absorber. Figure 3.3 gives a table of the Aeroflex Isolator performance. The ones to be used are the C2-H-710's.

FIGURE 3.2 Photograph of an Aeroflex Isolator.

FIGURE 3.3 Aeroflex Isolator performance tables.

3.1. ENGINEERING DESIGN FOR SHOCK AND VIBRATION ISOLATION

Let ω_b denote the servo-system bandwidth. Let ω_r denote the resonant frequency of the isolation system. Then the following rule can be used:

$$\omega_b > 4\omega_r \tag{3.1}$$

$$\omega_r = \sqrt{\frac{Kg}{W}} \tag{3.2}$$

where

K = total spring constant of the isolators (lb/in).

g = 386 in/sec^2

w = weight of the internal mounting board (lb).

Sufficient weight will be attached to the internal mounting board so that (3.1) is satisfied.

3.2. MECHANICAL CONSTRUCTION OF THE PHOTO-OPTIC ASSEMBLY

Figures 3.4 and 3.5 illustrate the vertical cross-sections of the photo-optic assemblies of the wayside and train terminals respectively. The horizontal cross-sections AA, BB, and CC illustrate the laser assembly, the photo-diode communication receiver assembly, and the servo system angular error detector assembly. The constructions of these assemblies are identical for both the train and wayside terminals, and are shown in Figures 3.6 to 3.8. We note in Figure 3.4 and 3.5 that the laser is on top while the signal receiver is at the bottom for the wayside terminals, and the reverse is true for the train terminal. In this way the laser of each terminal is on the same horizontal plane with the communication receiving photo-diode of the other terminal. While there is some vertical misalignment for the servo horizontal angular error detectors, the reduction in signal strength is immaterial because the servo bandwidth is much lower than the communication bandwidth. The noise power in the servo error signal is proportionally lower than the noise power in the communication signal. With the three reflectors lined up vertically on the same servomotor shaft, the servo beam direction is also lined up with the error detector null direction, and the most sensitive direction of the communication photo-diode.

Figures 3.6 to 3.8 illustrate the arrangements at the three levels A-A, B-B, and CC respectively. When the reflectors are facing the central dividing or reference line O-R, the laser beam is reflected to the center of its window in A-A, and incident light beams perpendicular to the windows would be concentrated to a focal neighborhood surrounding the photo-diode at D in B-B, and the dividing partition at P in C-C. When the servo shaft is moved by a small angle θ from its reference position, the laser beam direction, incident light directions

for maximum sensitivity in B-B, and zero error output in C-C would move by the same angle of 2θ.

An error detecting light storage box EB is shown in Figure 3.8. EB is partitioned into two light storage boxes with light scattering white walls in the interior, one opening at the partition to admit the focused incoming light, and two small holes in the rear for exposure of the error detecting photo-diodes. The differential voltage between the diode outputs is the error signal.

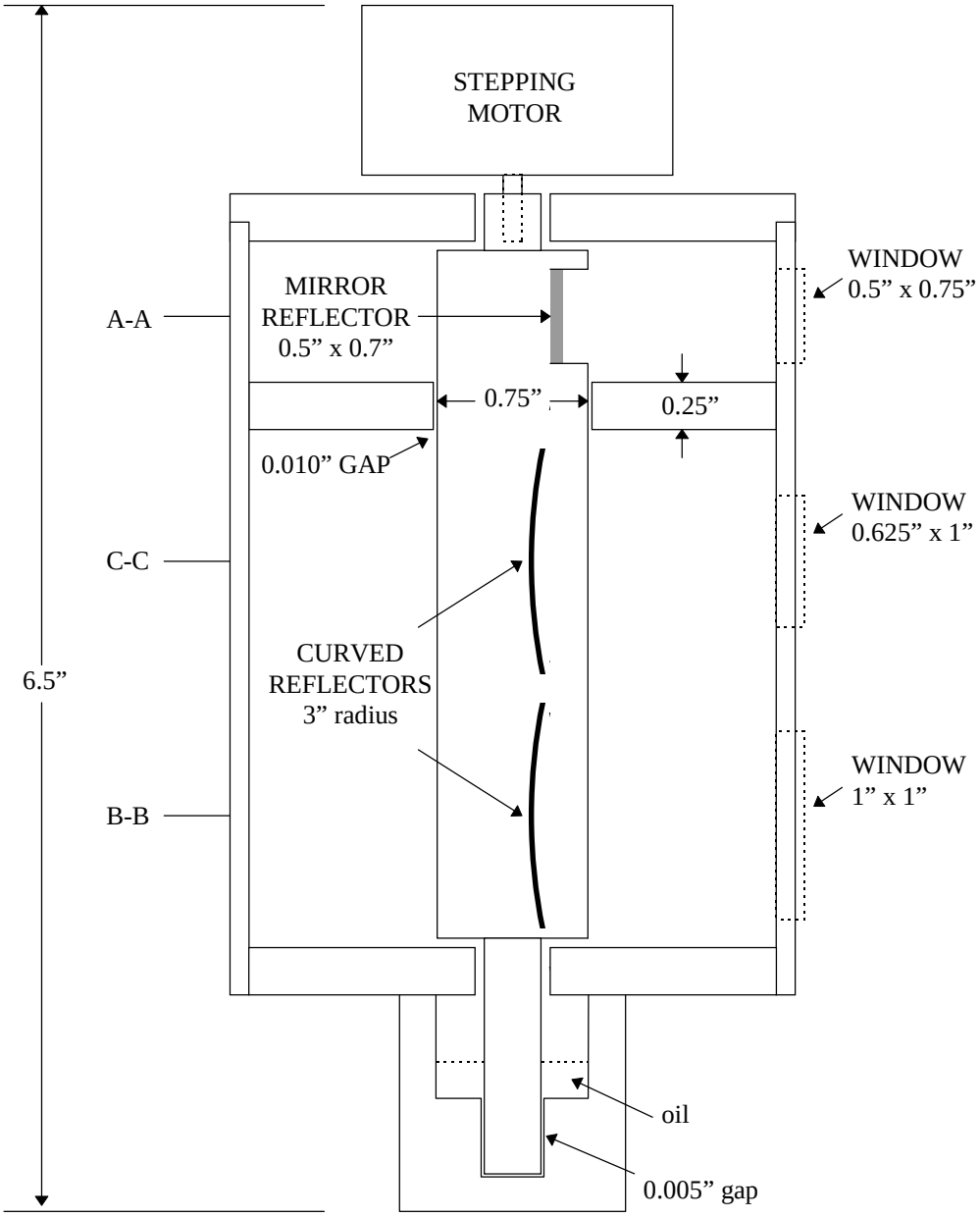

FIGURE 3.4 Vertical cross-section of the wayside terminal photo-optic assembly.

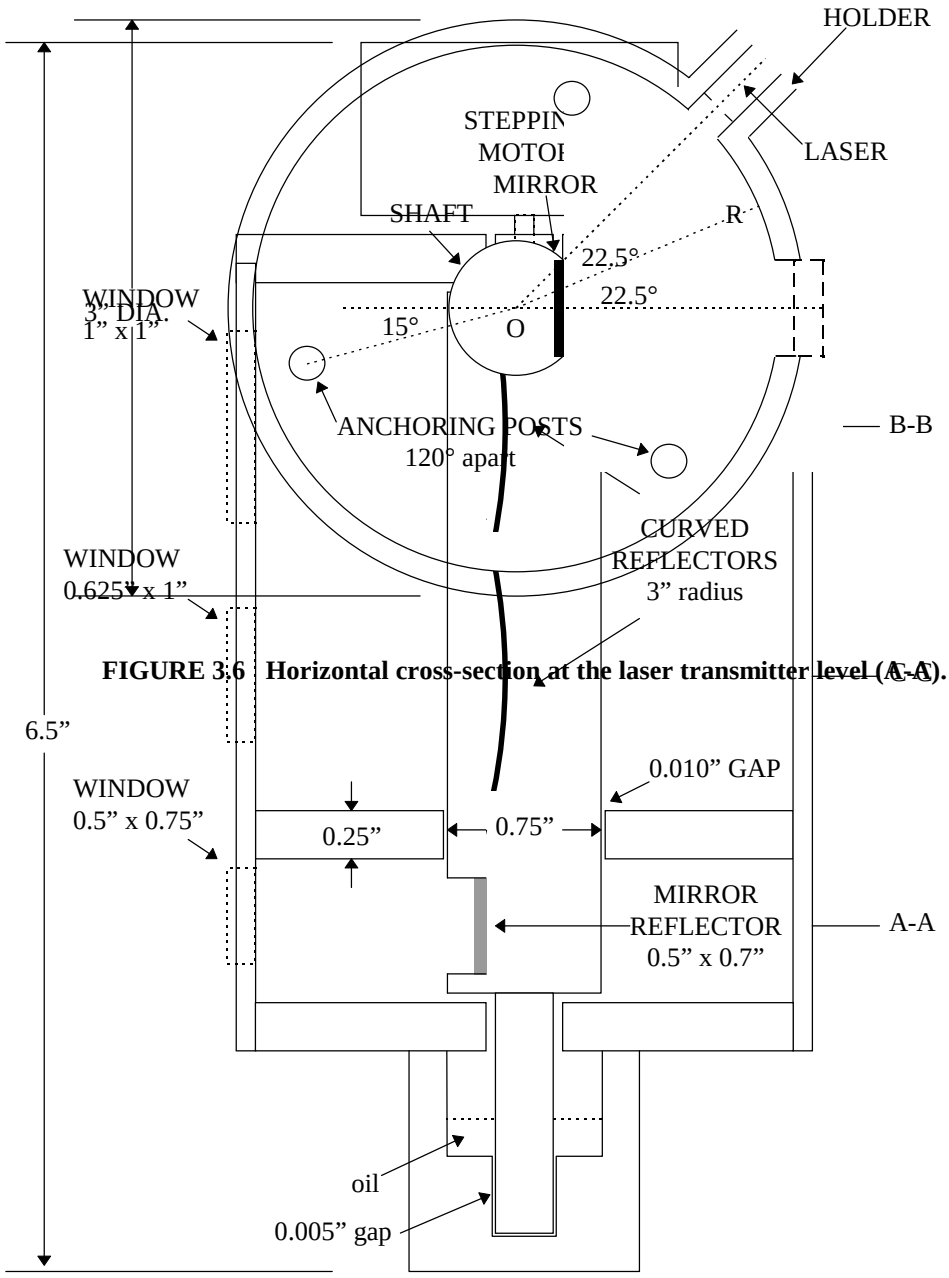

FIGURE 3.6 Horizontal cross-section at the laser transmitter level (A-A).

FIGURE 3.5 Vertical cross-section of the train terminal photo-optic assembly.

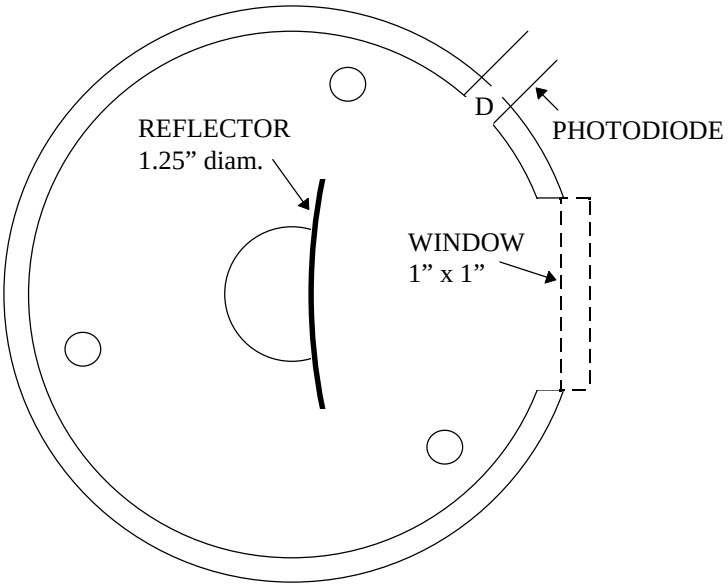

FIGURE 3.7 Horizontal cross-section at the communication signal receiver level (B-B).

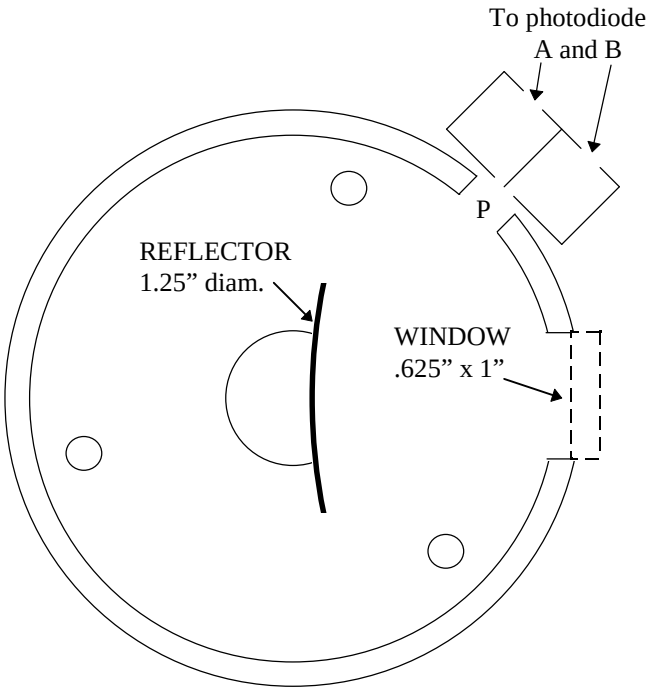

FIGURE 3.8 Horizontal cross-section at the servo error detector level (C-C).

4. OPTICAL DESIGN

We shall use dark red laser light (0.67 μm) for experimental work. With slight defocusing, the beam divergence can be adjusted to 0.01 radian, full angle. An average laser output power of 5 mW is used.

We design for the condition that communication starts at a distance between terminals of 30 meters, and ends at a distance between terminals of 10 meters.

4.1. HORIZONTAL OFFSET ANGLE

The terminals are set at a distance of 1 meter apart horizontally. At 30 meters, the offset angle is 1.91°, and at 10 meters, the offset angle is 5.71°, giving an angular difference of 3.8°. Thus a light beam movement angle of ± 2° is more than adequate to cover the offset angular difference. Correspondingly, a servomotor range of movement of ± 1.0° is required.

4.2. MAXIMUM AND MINIMUM PEAK LIGHT INTENSITY

The peak light intensity is given as:

$$I = \frac{5\ \text{mW}}{\text{duty cycle}} \times \frac{e^{-\gamma d}}{\text{beam area}}$$

where d is distance and γ is an attenuation factor. At a distance of *10m*, without rain, snow, or fog, $\gamma = 0$, and the beam area is:

$$\frac{\pi}{4} \times (1000 \times .01)^2 = 78.54 \text{ cm}^2$$

The duty cycle is approximately 0.5. Thus:

$$I_{\max} = \frac{0.005}{0.5} \times \frac{1}{78.54} = 127.3 \text{ mW/cm}^2$$

$I_{\min}$, minimum intensity, occurs at a distance of 30 meters under heavy fog. The attenuation coefficient is 0.0314/meter. Thus:

$$I_{\min} = \frac{I_{\max}}{9} \times e^{-0.942} = 5.514 \text{mW/cm}^2$$

4.3. CURVED REFLECTORS

Each curved reflector has a radius of approximately 6" and concentrates the received light to a focal area of approximately 0.25" at the reception point. Its light intensifying factor is estimated as

$$F_i = \left(\frac{1.25}{0.25}\right)^2 = 25 \qquad (4.1)$$

Another factor is the light reflection and attenuation as it passes each of the four glass windows of Figure 3.1. Since the light beams are nearly normal to the glass surfaces, the attenuation is low. The overall attenuation is estimated as

$$F_a = 0.9^4 = 0.66 \qquad (4.2)$$

5. SERVOMOTOR FEEDBACK CONTROL SYSTEM

There are two subsystems for the servomotor feedback control system:

(i) generation of the actuating error signal, and

(ii) nonlinear servomotor drive system.

5.1. GENERATION OF THE ACTUATING ERROR SIGNAL

Generation of the actuating error signal is explained in four parts, detailed in subsections 5.1.1, 5.1.2, 5.1.3, and 5.1.4.

5.1.1. Photo-detector With Amplifier

Two Devar 529-2-5 are used as the photo-detectors illustrated in Figure 3.8. Each unit has a built-in operational amplifier with sufficient gain and bandwidth. Figure 5.1 and Tables 5.1 and 5.2 illustrate the schematic and engineering data of the Devar 529-2-5. Figure 5.2 illustrates the external connections.

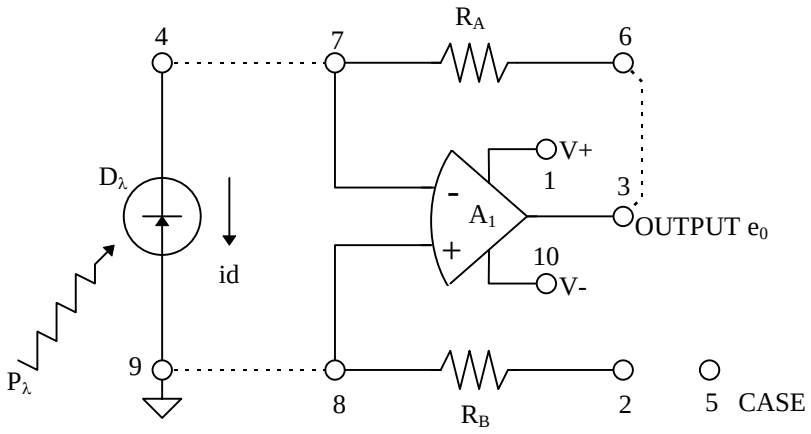

FIGURE 5.1 Schematic data of Devar 529-2-5.

TABLE 5.1					
PARAMETER	SYMBOL	-1	-5	UNITS	CONDITIONS
Diode Responsivity	$K\lambda$	0.6	0.6	$\frac{\text{Amperes}}{\text{Watts}}$	$\lambda = 0.9 \times 10^{-6}$ m.
Lunimous Responsivity	$K\lambda_{(L)}$	8.5	8.5	mA/lm	T_s = 2854 °K
Resistance	R_d	140×10^6	50×10^5	Ohms	
Capacitance	C_d	15×10^{-12}	45×10^{-12}	Farads	
Dark Current	I_d	2×10^{-9}	5×10^{-9}	Amperes	V_d = -15 V
Active Area	A_d	0.8	5.0	mm^2	
Active Dia.	ϕ_d	1.0	2.52	mm	
Reverse Bias Voltage	$-V_d$	0-45	0-45	Volts	Limits
Max. Allowable Irradiance	I_{max}	.03	.03	$\frac{\text{Watts}}{mm^2}$	Steady State

Photodiode Characteristics: (V_d = 0V, T_A = 25 °C, unless noted)

TABLE 5.2				
PARAMETER	SYMBOL	VALUE—80 PERCENTILE	UNITS	CONDITIONS
Input Bias Current	I_B	2×10^{-9}	Amperes	
vs. Temp.	dI_B / dT	-1×10^{-11}	A/°C	
Input Offset Voltage	E_{OS}	$\pm 5 \times 10^{-3}$	Volts	
vs. Temp.	dE_{OS} / dT	$\pm 10 \times 10^{-6}$	V/°C	
Open Loop Unity Gain Cross Over Frequency	fx	2×10^{6}	Hz	Small Signal
Slew Rate Limit	de_0/dT	5×10^{5}	V/Sec.	e_0 = 20V P-P
Output: Current	I_0	$\pm 5 \times 10^{-3}$	Amperes	$R_L = 2 \times 10^3 \Omega$
Voltage	V_0	± 10	Volts	$R_L = 2 \times 10^3 \Omega$
Supply: Current	$\pm I_S$	1×10^{-3}	Amperes	$V_S = \pm 3$ to 18V
Voltage	$\pm V_S$ Min. $\pm V_S$ Max.	3 18	Volts Volts	
Input Resistance	R_i	40×10^6	Ohms	

Amplifier Characteristics: ($V_S = \pm 15V$, $T_A = 25°C$, unless noted)

Let V_7 and V_3 denote the voltages at 7 and 3 where respectively. The following nodal equations are obtained:

$$\left(G + Cs\right)V_7 - \left(\frac{1}{R} + C_f s\right)V_3 + I_d = 0 \qquad (5.1)$$

$$V_3 = -\frac{K}{s}V_7 \qquad (5.2)$$

$$G = \left(\frac{1}{50} + \frac{1}{40} + \frac{1}{R}\right) \times 10^{-6} + \frac{1}{R_i} \qquad (5.3)$$

$$C = 45 \times 10^{-12} + C_i \qquad (5.4)$$

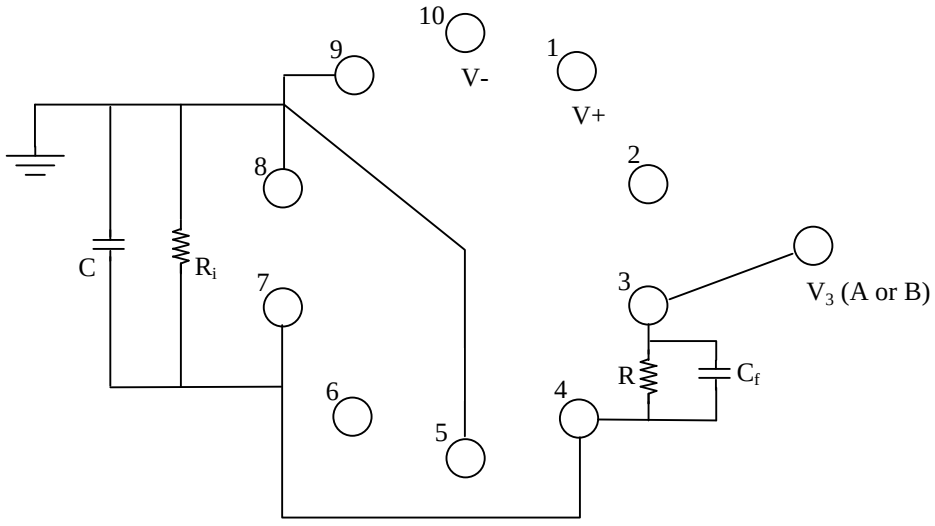

FIGURE 5.2 External connection of servo error photo-detector.

$$K = 2\pi \times 2 \times 10^6 = 12.57 \times 10^6 \quad (5.5)$$

Eliminating V_7 from (5.1) and (5.2) gives

$$\left[1 + \left(RC_f + \frac{RG}{K}\right)s + \left(\frac{RC}{K}\right)s^2\right]V_3 = RI_d \quad (5.6)$$

Equation (5.6) gives a low frequency gain,

$$V_3 = RI_d \quad (5.7)$$

bandwidth,

$$\omega_o = \left(\frac{RC}{K}\right)^{-\frac{1}{2}} \quad (5.8)$$

and damping factor:

$$\varsigma = \frac{\omega_o R}{2K}\left(G + KC_f\right) \quad (5.9)$$

Equation (5.7), (5.8), and (5.9) mean that the low frequency gain can be determined by specifying *R*, the bandwidth can be determined by specifying C_i, and the damping factor can be selected by specifying C_f and *G*. However, a higher *G* means more dissipation of the signal power. Thus, we set $R_i = 0$, $R = 200K$, $C_i = 0.5\ \mu$F, and $C_f = 600$ pF. Equations (5.8) and (5.9) give:

$$\omega_0 = 1.12x10^4 \text{ rad / sec} \quad (5.10)$$

$$\varsigma = 0.67 \quad (5.11)$$

5.1.2. Correction For Transducer Gain Dependence On Distance And Weather Condition

The photo cell system is a transducer which converts angular error to an output voltage $V_{3A} - V_{3B}$, where the subscripts A and B denote the two photo-detectors of Figure 3.8. Referring to (5.7), the two voltages are proportional to the photo-diode currents $I_{d\text{A}}$ and $I_{d\text{B}}$, which are in turn proportional to the incoming light intensity. Referring to section 4.2, under different weather and train distance conditions, the maximum and minimum light intensity values can vary over a range of

$$\frac{I_{\max}}{I_{\min}} = \frac{127.3}{5.514} = 23$$

The above ratio means a closed-loop gain variation of

20 log 23 = 24dB

and it would make stabilization of the closed-loop system difficult.

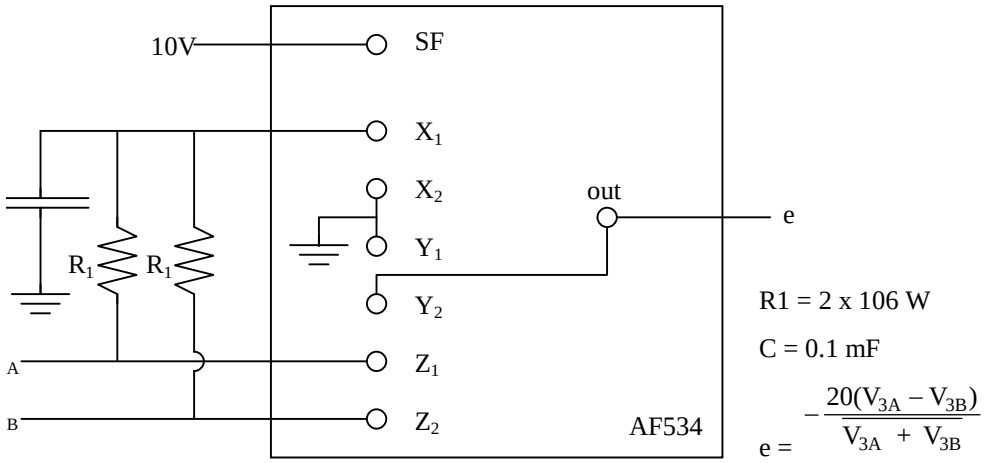

FIGURE 5.3 AD534 divider circuit for automatic gain regulation.

The transducer gain variation is eliminated by using the AD534 multiplier circuit as a divider circuit as shown in Figure 5.3. The AD534 output can be written as

$$e = A\left[\frac{(X_1 - X_2)(Y_1 - Y_2)}{SF} - (Z_1 - Z_2)\right] \tag{5.12}$$

With the circuit connection of Figure 5.3, we have:

$$X_1 - X_2 = \frac{1}{2}(V_{3A} + V_{3B}) \tag{5.13}$$

$$Y_1 - Y_2 = -e \tag{5.14}$$

$$Z_1 - Z_2 = V_{3A} - V_{3B} \tag{5.15}$$

In (5.13) the average value of V_{3A} and V_{3B} is obtained by filtering through an *R-C* filter with a 0.1 sec time constant. It is sufficiently fast to follow the change in average V_3 as the train moves. Substituting (5.13) (5.14), and (5.15) into (5.12) and solving for *e* give

$$e = \frac{V_{3B} - V_{3A}}{\frac{1}{A} + \frac{1}{2 \cdot SF}(V_{3A} + V_{3B})} \tag{5.16}$$

As *A* is a very large gain constant, neglecting $\frac{1}{A}$ gives:

$$e = V\frac{2 \cdot SF(V_{3B} - V_{3A})}{V_{3B} + V_{3A}} \tag{5.17}$$

5.1.3. The Differential Light Storage And Sensing Chamber

In our previous design, the two photo-diodes for generating servo error signal were placed side by side. Because of the physical dimensions of the two diodes, a

dead zone of approximately 0.3" between the diodes was created. The error signal is shown in Figure 5.4(a).

In our new design, a light sensing and storage chamber is interposed between the light beam and the photo-diodes as shown in Figure 3.8. The error signal is illustrated in Figure 5.4(b). The system now operates well because any slight error from neutral would generate a large restoring torque.

5.1.4. An Error Integration Network

The error integration network is illustrated in Figure 5.5. Its function is to stabilize and optimize the servo control loop by integrating the error *e* with time to a substantially larger actuating error *a*. An analysis similar to that of 5.1.1 gives the network transfer function as:

$$\frac{A(s)}{E(s)} = \frac{R_3}{R_1} \cdot \frac{1 + R_2 Cs}{(R_2 + R_3)Cs} \qquad (5.18)$$

Equation (5.18) shows that with a sufficiently large R_3, a larger actuating error *a* can be generated with a negligibly small residue error *e*.

5.2. ON-LINEAR SERVOMOTOR DRIVE SYSTEM

In our previous designs, the stepping servomotor which we used was the Kollmorgen PF25-24. The motor was much too small, with an outside diameter of 0.984 inches and a holding torque of 1.11 oz-in. The reason why we used such a small motor was that the PF25-24 was the only available stepping motor with n=24, where n is the spatial cycle per revolution. All larger motors have an n value of *48* or higher. This is easy to understand. Stepping servomotors are used mostly for numerical drives. The angular displacement per step θ_1 is given by

$$\theta_1 = \frac{360^\circ}{n} \qquad (5.19)$$

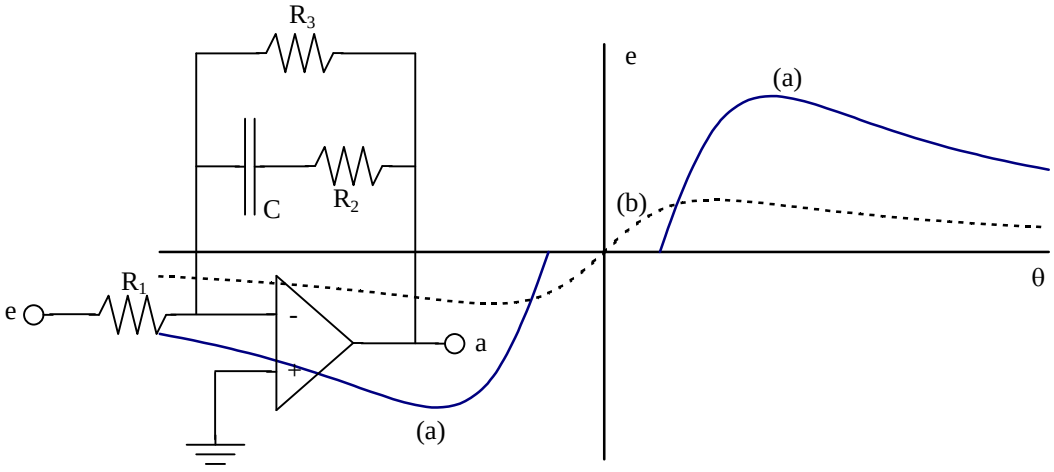

FIGURE 5.4 Effects of differential light sensing and storage chamber.

FIGURE 5.5 An error integration network.

Larger *n* means finer steps, and it is therefore preferred by the numerical tool industry. We selected a stepping motor for a different reason: it is simple in construction, without radio noise, and is equivalent in its performance to an a.c. servomotor with an *n*:1 frictionless reduction gear train. However, its nearly linear range for beam deflection angle is no more than $\theta_1 / 2$. With *n=48*, the nearly linear beam deflection range is 3.75°, which is insufficient for our application. Our initial effort was to order a larger stepping motor with *n*=24: PF42-24. After two months of waiting, we received the PF42-48 instead. The PF42-24 motor was apparently discontinued.

Then we worked out a non-linear drive circuit, and decided to give it a try. Both the reference phase current and control phase current depend on the actuating error *a*, as illustrated in Figures 5.6 and 5.7. The beam deflection angle's nearly linear range was extended beyond $\theta_1 \diagup 2$ as expected. A comparison of the three motors' performances is given below in Table 5.3.

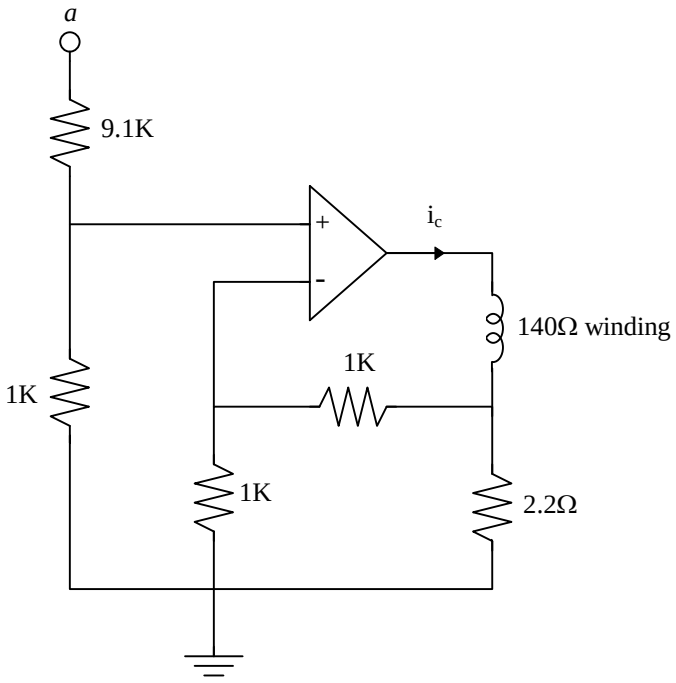

(a) control phase

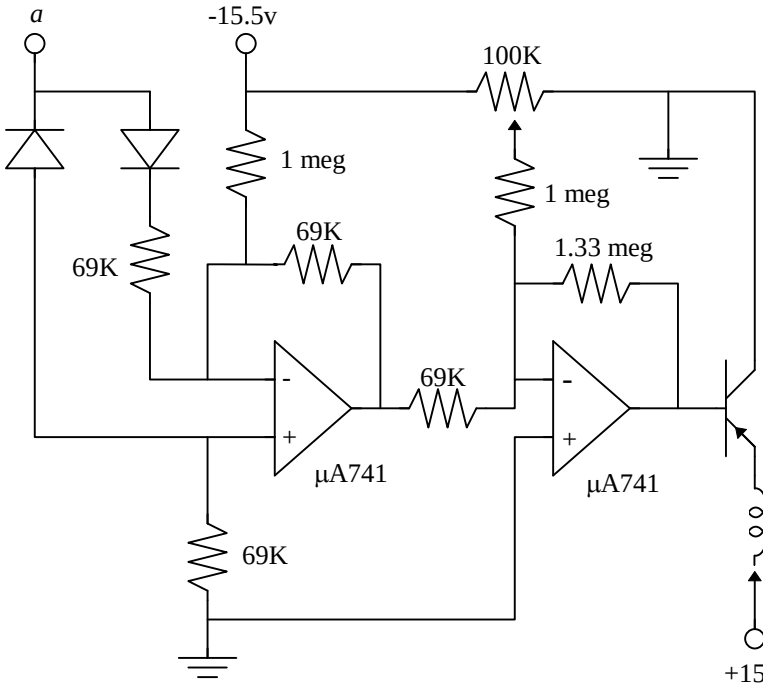

(b) reference phase

FIGURE 5.6 Servomotor driving circuits.

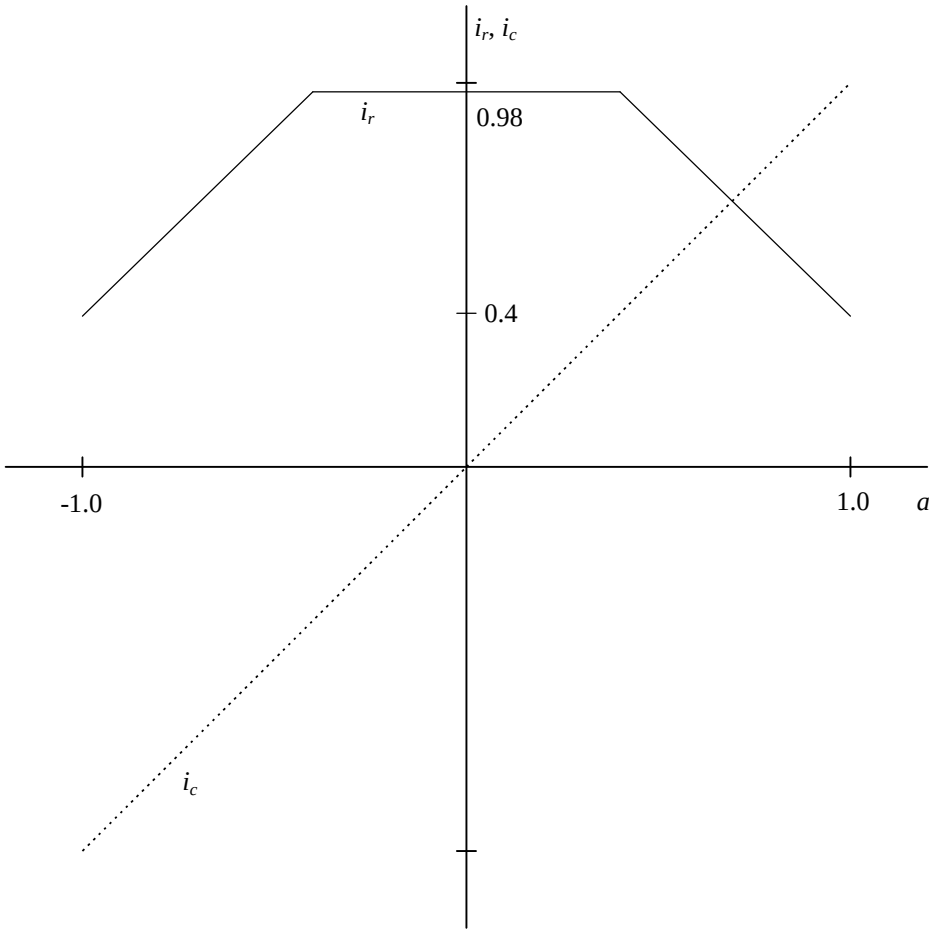

FIGURE 5.7 Control and reference phase motor currents, i_c and i_r, versus actuating error a.

TABLE 5.3

Motor	Drive circuit	Torque (oz-in)	Beam deflection range
PF25-24	Linear	1.11	7.5°
PF42-24*	Linear	4.17	7.5°
PF42-48	Linear	6.25	3.75°
PF42-48	New	6.25	6.5°

* No longer available on the market, at least in our experience.

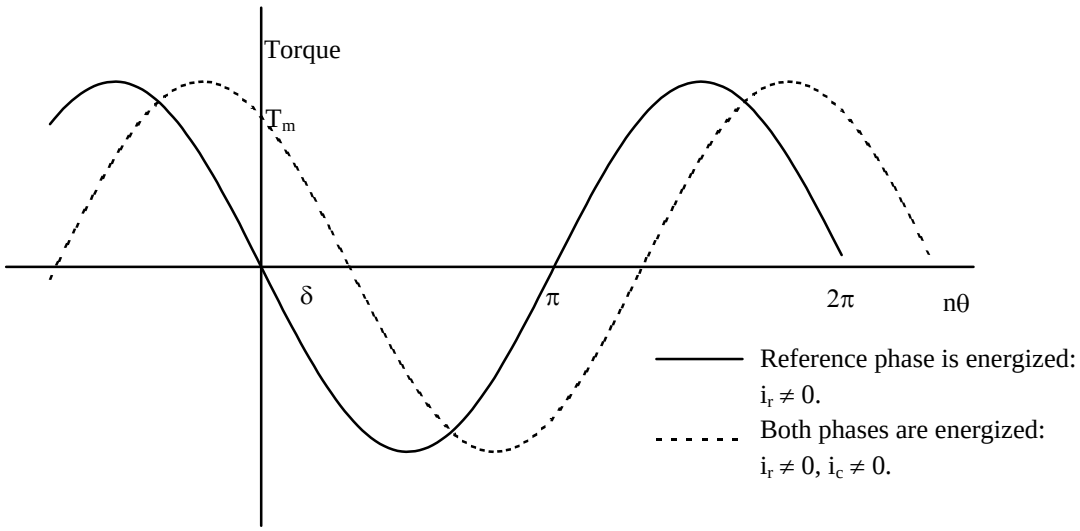

FIGURE 5.8 Motor torque versus shaft angle (electrical).

The new drive circuit not only solved the shortage of supply problem, it also increased the torque by 50%. To our knowledge, the new drive circuit has not been published, nor used elsewhere.

5.2.1. An Analysis Of the Non-linear Drive System

Figure 5.8 illustrates the torque versus motor shaft position angle θ for a stepper servomotor. The solid curve illustrates the case in which only the reference phase is energized: $i_c = 0$. The shaft is at a stable equilibrium position with $\theta = 0$, and at an unstable equilibrium position with $\theta = \pi / n$. The broken curve illustrates the case in which the control phase is also energized. Then:

$$\delta = \tan^{-1}\frac{i_c}{i_r} \tag{5.20}$$

$$i = \sqrt{i_r^2} + i_c^2 \tag{5.21}$$

$$T_m = Bi \tag{5.22}$$

where δ is the shift in equilibrium position, i is the resultant current, and T_m is the maximum torque as illustrated in Figure 5.8. The constant B is characteristic of the stepping motor. It depends on the airgap geometry, the maximum flux density, and the number of turns of each winding. Using the above results, a plot of δ and T_m versus a is illustrated in Figure 5.9. To produce a beam angular movement of ± 2°, we need only a range in δ of ± 48°. It is well within the nearly linear range of Figure 5.9.

6. LIGHTWAVE TRANSMISSION AND RECEPTION

After careful considerations we decided to use a red laser in one direction, and an infra-red laser (1.55 micron, and 0.002 watt average light power) in the opposing direction. The reasons are as follows:

(i) Two different light frequencies must be used so that during rain or snow the reflected light would not interfere with received light from the other terminal for both the servo error signal and the communication signal.

(ii) Optical filters for two visible lightwave signals are costly in terms of both money, and transmitted signal fidelity, if the filters are to the sufficiently effective in separating the two lightwaves.

(iii) Lightwaves at the shorter visible wavelengths are very harmful to human eyes.

In contrast the infra-red lightwave as specified

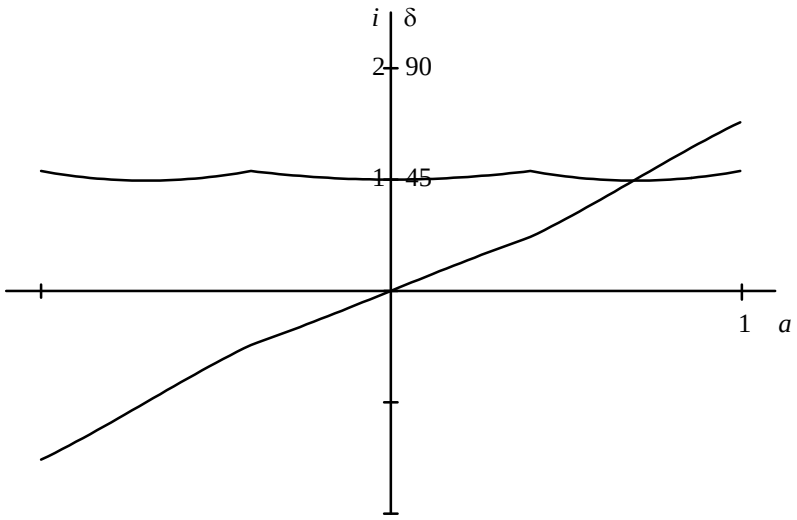

FIGURE 5.9 Equilibrium position shift δ and maximum torque T_m versus actuating error

above is completely safe for human eyes. Light filters are not needed. Infra-red lightwave does not have sufficient quantum energy to kick an electron over the energy gap of a visible light detector, and infra-red lightwave detectors are very insensitive to visible lightwaves because of the large bandwidth separation.

6.1. INFRA-RED TECHNOLOGY

There were two developments in infra-red technology:

(i) Infra-red lightwave is not visible. To determine its radiation pattern, we developed an infra-red detection array.

(ii) Infra-red reflective surface is very different from visible light reflective surfaces, and there is no continuity. For instance, both white and red surfaces are strong absorbers of infra-red light. The only good surfaces, which we found for reflecting infra-red, are gold plated surfaces. These give almost 100% reflection of infra-red light. By using only gold-plated surfaces for reflecting infra-red lightwaves, we improved the signal to noise by approximately 20 dB. Now the signal transmission in both directions are equally good.

6.2. LIGHT TRANSMITTING AND RECEIVING CIRCUITS

Our effort in developing high speed transmitting and receiving electronics was limited by the frequency response of commercially available operational amplifiers.

Figure 6.1 illustrates the laser driver circuit. A single stage amplifier (Q_1) is used as the signal amplifier. A μA741 (Q_2) and an npn transistor (Q_3) are used for laser radiation intensity control. If the laser intensity exceeds a preset limit, the built-in photo-diode would deliver positive current to the negative terminal of Q_2. A negative

voltage would be produced at the output of Q_2 and reduce the negative d.c. current which is supplied through Q_3 to the laser.

Figure 6.2 illustrates a receiving circuit using an Analog Modules transimpedance amplifier. The diode is coupled directly into the input terminal of the amplifier for both the red and infra-red lightwaves. YAG-200A is used for detecting the red light at 0.67 micron wavelength and C30641G used for detecting the infra-red light at 1.55 micron wavelength. The two detectors are mutually insensitive. Each of the photodetectors is coupled directly to an Analog Modules 312A-4 transimpedance amplifier, which has a frequency response from 200 Hz to 200 MHz

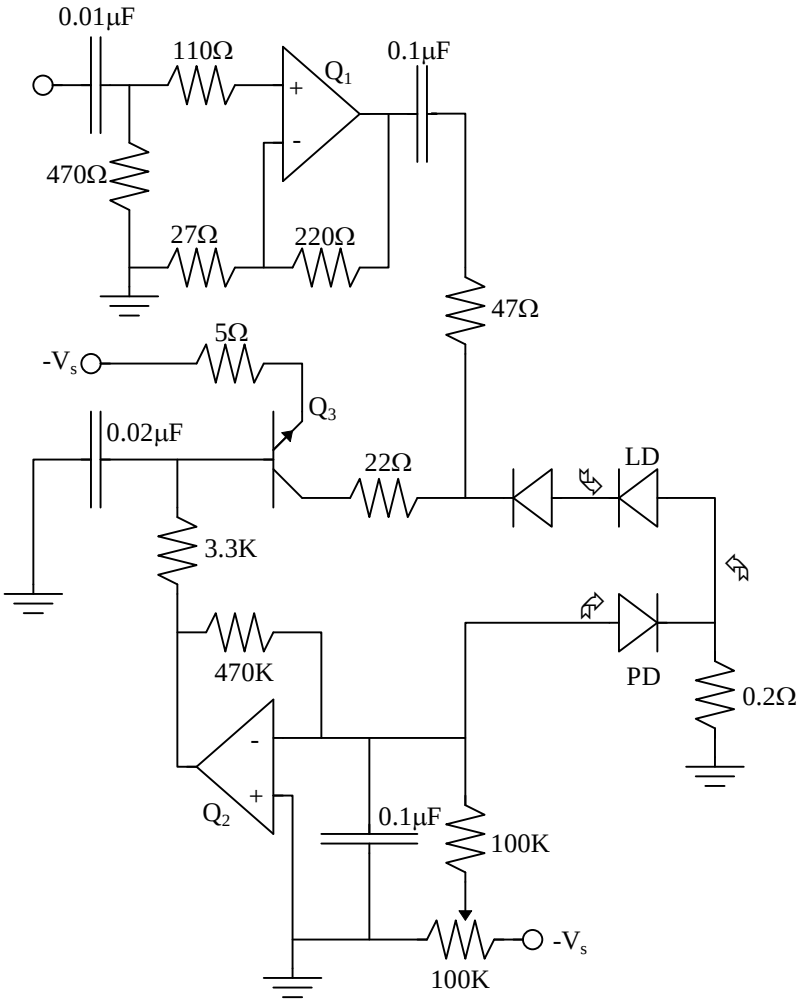

FIGURE 6.1 Laser transmitter driver circuit.

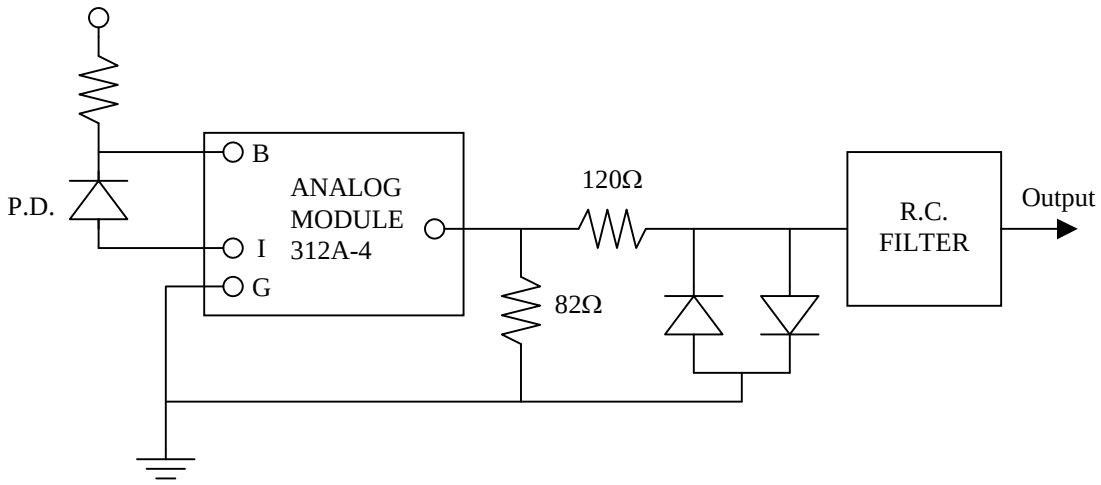

FIGURE 6.2 Photo-receiver with transimpedance amplifier.

and a transimpedance gain of 1 volt per microampere. Its output is coupled to a pair of silicon diodes through a 120Ω resistor. The diodes clamping circuit limits the amplifier to approximately ± 1.6 volts, which is the operating voltage range of the Ethernet card input. However, the Ethernet card electronics is extremely sensitive to the high-frequency harmonies generated at the four corners of the diode clamping circuit, and a low-pass R.C. filter is used to reduce the harmonies above 20 MHz.

7. COMMUNICATION COMPUTER

In discussions with the Long Island Railroad, we came to the consensus that for a railroad application, the best solution is to use a standard high-speed microcomputer. These computers are sufficiently versatile to satisfy all the following needs:

(i) Various train control, communication, position and speed determination, etc., tasks,as described in Section 7.1, can be easily programmed in software.

(ii) The time delay for train control in an emergency is no more than a few microseconds. It is a few orders of magnitude less than human response time. Even the fastest train moves less than 1 cm in this time period.

(iii) A standard microcomputer has far more than sufficient memory for information storage and forward. The transmitted information is stored both ways in each encounter of the IDEA-LOOC train terminal with an IDEA-LOOC wayside terminal. The stored information is then digested and used in leisure.

(iv) Standard microcomputers can be purchased and stored in quantity in negligible cost in terms of railroading money. One need only add specialized software before putting it into service.

In section 7.1, we assume that a standard microcomputer is used, and the material in Section 7.1 is a description of its software and firmware functions.

7.1. COMMUNICATION COMPUTER FUNCTIONS

Figure 7.1 illustrates a block diagram of the communication computer (CC) for full two way communication. The way the system operates is described below:

(i) Before the train reaches x_1 (the distance at which communication commences) the messages to be transmitted are sent by the Train Computer or Wayside Computer through the Serial I/O Device and stored in the Transmitting Message section of the CC Main Memory.

(ii) The CC Microprocessor computes the byte parity checks (BPC) of each byte of the message to be transmitted, and stores it in the transmitting parity checks section of the CC Main Memory (TPC).

(iii) A 32-bit microprocessor will be used as the CC Microprocessor. A coding unit or word group has 2^n message words, where n is usually between 4 and 6; 2^{n-3} check words from the BPC's; a vertical bit by bit

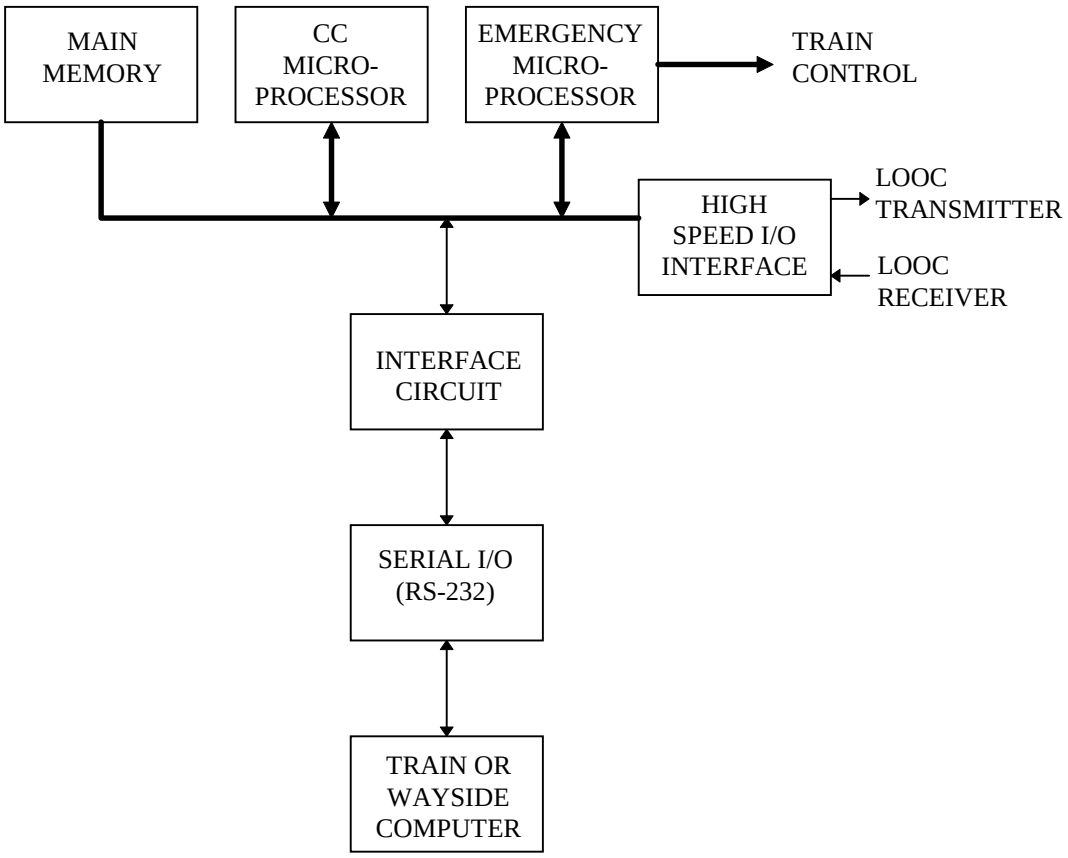

FIGURE 7.1 LATCC communication computer.

check word for the 2^n message words, and a vertical bit by bit check word for the 2^{n-3} BPC formed check words. Thus, the total number of words in a group is:

$$N_g = 2^n + 2^{n-3} + 2 \qquad (7.1)$$

In a message of 2 megabytes, the number of word groups is:

$$N_c = \frac{2x2^{20}}{2^{N+2}} = 2^{19-n} \qquad (7.2)$$

For instance, with 64 message words in a group, the number of word groups in a message of 2 megabytes is $2^{13} = 8{,}192$. The $2^{n-3} + 2$ parity check words are stored in the TPC section of the memory.

(iv) As the train terminal arrives within the distance $x_1 \le x \le x_2$ of the wayside terminal, message transmission begins in the order of word groups. For each group, the transmitting terminal sends the message words first and then the parity check words.

(v) The receiving terminal computes the parity check words from the received message words and XORs them with the corresponding received parity check words. If the result is "0" everywhere, the receiving terminal sends back a highly redundant "acknowledgment". The transmitting terminal begins to transmit the next word group upon receiving the "acknowledgment". Otherwise it repeats the unacknowledged word group.

(vi) Some microprocessors have built-in hardware for automatic byte parity checks and 32-bit word-wide XOR machine instructions. The automatic byte parity checks can be in the microprocessor itself or in its associated system bus. Intel 486 and Pentium processors are within this group. Using one of these microprocessors, the acknowledgment processing and transmitting time including round trip delay is of the order of one percent of the word group transmission time.

(vii) In the same set of highly redundant signals, the alternatives to "acknowledgment" are "repeat", "interrupt", and "direct control".

"Repeat" means that parity check error(s) have already been discovered. The transmitting terminal is to repeat the word group being transmitted immediately from the very beginning.

"Interrupt" means that the receiving terminal is to start transmitting, and the transmitting terminal is to change to receiving status.

"Direct control" means that the receiving terminal is to start transmitting word groups of control signals. The transmitting terminal is to change to receiving status and to send the first

few (a fixed numbers) received word groups to Control Interface.

(viii) There is a set of two highly redundant signals from the transmitting end: “end of message”, and “direct control”.

(ix) Software for carrying out the above protocol is to be in a Local Memory of the CC Microprocessor.

8. ARRANGEMENT WITH THE LONG ISLAND RAILROAD (LIRR)

In our continuing work, we have reached the following arrangements with the Long Island Railroad:

1. The wayside terminal is to be installed on the Babylon Tower, and the train terminal is to be installed on the Track Geometry Test Vehicle TC-81. In testing the terminals Vehicle TC-81 can approach the Babylon Tower at any desired speed up to 40 MPH.
2. Stony Brook will provide the ready-for-installation test terminals. The LIRR will absorb the installation cost and provide the installation personnel.
3. The test and demonstration period can be as long as six months. During this period, Stony Brook will be responsible for maintaining the terminals in good working order. The LIRR will absorb all other cost.

The Babylon Tower is a major control tower of the LIRR with monitor and control equipment and hundreds of track circuits wired into the control room. Vehicle TC-81 is used by LIRR for observing the track conditions, especially track wear, of the entire LIRR railway system. With a very powerful scanning laser mounted underneath the vehicle, it can collect millions of bytes of information about the track as the vehicle runs from one station to another. The LIRR is interested in eventually using our LOOC device for downloading the collected information at each station as TC-81 passes.

9. USE OF STANDARD DELL COMPUTER

Because of cost limitations, two DELL computers, instead of the special purpose communication computers described in Section 7, are used for the present project. The DELL computers are adequate for testing at LIRR to down load the collected information at each station as TC 81 passes.

Figure 9.1 illustrates the way two DELL computers are interconnected with a 50 Ω cable. An ethernet card is inserted at each end between the computer and the cable. At the input end, the ethernet card is to match the computer output electrical signal to the cable requirements, and vice versa at the output end. In actual operation LOOC linkages are used for both ways instead of the cable. The two ethernet cards remain in place at the computer terminals without change.

A working model was demonstrated at NAS on Nov. 17th, 1998.

10. CONCLUSION

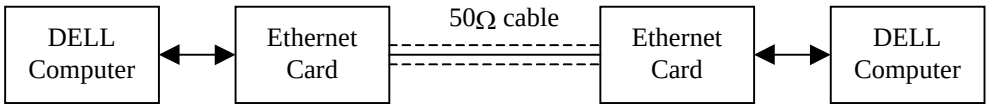

FIGURE 9.1 Interconnection of two DELL computers (LOOC electronics take the place of the cable).

Direct lightwave communication between train and wayside terminals is a vital link in the modernization of railroad operations. Potential applications include the following:

On Line Servicing of Vehicles:

In many railroad operations, diagnostic signals for various parts and devices are collected and stored in an on-board microprocessor CPU when the train is in motion. These signals are used for maintenance at a later time. With train-to-wayside communication links, such signals can be conveyed to a wayside terminal before entering a major station so that the cars that need servicing can be either switched off or serviced on line.

Train Control Systems:

There is an increasing need for the rapid exchange of large data files between high-speed trains and wayside facilities. One example is the data exchange requirements of communications-based train control systems. These systems require downloading and uploading of large data files such as track and route characteristics, and train consist data. Conventional data radio links may not always be the most effective means for such data exchanges, due to factors such as data volume, interference, and communications coverage problems.

Passenger Services:

Because of its high information transmission rate, LATCC offers opportunities to make a significant difference to the train's information service. Passengers on a train not only will have up to date information on immediate intermodal transportation, they can also select and book the next leg of their journey.